MATEJ KRPAN   **IGOR KUZLE**

matej.krpan@fer.hr   igor.kuzle@fer.hr

University of Zagreb Faculty of Electrical Engineering and Computing

THE MATHEMATICAL MODEL OF A WIND POWER PLANT AND A GAS POWER PLANT

SUMMARY

To enable conduction of quality research of power system dynamics using computer simulation software, appropriate mathematical and simulation models have to be developed. In the last two decades, an exponential increase of installed wind power capacity can be observed, while the gas power plant capacity and energy production has also seen an increase in the recent years. Consequently, their impact on power system dynamics is no longer negligible. Furthermore, the increased penetration of wind power has led to a lot of research concerning frequency support capabilities from wind power plants (WPPs). In this paper, after a brief theoretical introduction, simplified system frequency response (SFR) simulation models of a generic wind power plant and a gas power plant have been developed in MATLAB. These generic models have been integrated with existing SFR models of a steam and hydro unit. The model contains a representation of under-frequency load shedding (UFLS) and demand response, as well. Graphical user interface (GUI) has been developed to control this expanded model.

Key words: wind power plant; gas power plant; primary frequency regulation; power system; MATLAB

1. INTRODUCTION

To reduce the carbon footprint of the power & energy sector, many countries throughout the world introduced various measures encouraging the integration of renewable energy sources (RES). The most popular energy sources for renewable power generation are the photo-voltaic (PV) plants and the wind power plants (WPPs): in 2016, installed PV capacity was 291 GW and installed WPP capacity was 467 GW in the world [1] and will continue to rise. On the other hand, United States Energy Information Administration predicts a grow of 2.1% per year for electrical energy generation from natural gas from 2015 to 2017 [2]. In the grid frequency control context, the turbine dynamics dictate the frequency response dynamics after a disturbance. More precisely, grid inertia dictates the rate-of-change-of-frequency (RoCoF) while the turbine dynamics associated with the governor dynamics and mechanical dynamics dictate the behavior of primary frequency response.

Most wind turbines today are converter-connected to the grid which ensures electricity production at nominal grid frequency independent of the actual rotational speed of the turbine. However, this effectively decouples the mechanical and electrical frequency of the wind energy conversion system (WECS) [3] which means there will be no inertial response from WPPs after a disturbance occurs. Coupled with the fact that WPPs do not participate in primary frequency control, the frequency stability of a power system is getting more and more jeopardized. To combat this issue, a lot research has been conducted to utilize the kinetic energy of the wind turbine blades and high controllability of variable-speed drives for frequency support. The overview of the aforementioned research has been extensively covered in [4]–[7].

Gas power plants have also enjoyed an increase in their share of total electricity production since new materials and technologies with better thermodynamic efficiency are being constantly developed. Furthermore, natural gas is the least carbon-intensive of all fossil fuels (carbon dioxide emissions are about half the rate of coal) and it is also attractive for new power plants because of low capital costs and relatively low fuel cost [2]. Gas power plants are usually utilized as peaking power plants but can also be used as load following power plants in systems with an insufficient capacity of hydro power.

Low-order system frequency response (SFR) model provides a simple framework for studying power system frequency changes by considering only the most dominant time constants in the power system in the time scale of inertial response and primary frequency response. Based on the concept of average system frequency, it gives a good-enough estimate of the grid frequency behavior. As this is a very well-known and widely used approach, it will not be discussed anymore. For further reading, refer to [8]. In most of scientific literature, SFR model of a power system is used where only one type of turbine is represented, usually steam or hydro turbine. Rarely is there a mix of different turbines represented, e.g. steam-hydro (e.g. [9]), while gas turbines are rarely used for simulations, e.g. [10]–[12]. Wind turbines have not been represented so far because they did not participate in frequency response. The goal of thesis [4] was to research the existing literature

and expand the steam-hydro SFR model [9] in the way that, finally, it includes a model of a gas turbine as well as a model of a wind turbine (with frequency support capability). In this paper, the most important results of [4] will be summarized and discussed. Rest of the paper is structured as follows: in section 2 an SFR model of a gas turbine is presented; in section 3 an SFR model of a wind turbine is developed which exploits pitch angle control for primary frequency control; in section 4 an expanded power system SFR model is presented which includes a wind, gas, steam and hydro turbine along with a UFLS scheme and a demand response (DR) representation in the SFR context. Some examples of simulations are shown here. Section 5 concludes the paper.

2. A GENERIC GAS TURBINE MODEL FOR SFR SIMULATIONS

Gas turbine development lagged behind steam turbine development foremost because of material limitations (gas is burning at higher temperatures) and technical complexity of the design. From the conceptual standpoint, the gas turbine is similar to a steam turbine in a way that the output power is controlled by valves which govern the fuel supply. General theory of operation, main components and different types of gas turbines and gas power plants have been succinctly described in [4]. Conclusively, it is not necessary to individually model different types of gas power plants (GPPs) for this application because the gas turbines are virtually identical in the context of dynamic response: combined-cycle power plants use separate gas and steam turbines while cogeneration plants and big GPPs use gas turbines with similar if not identical dynamic properties.

A typical gas turbine model for power system stability studies is shown in Figure 1. According to Figure 1 [11], the control design consists of three control circuits: temperature control, speed control and acceleration control. To simplify the model even more, temperature and acceleration control will be ignored. The reasoning behind this simplification lies in the fact that these control circuits are active during abnormal conditions: temperature controller keeps the turbine blades from damaging when the temperature in the combustion chamber is too high by limiting the fuel supply. Acceleration controller is usually only active during start-up and shut-down. The temperature is assumed to be always in the normal range and that the turbine is operating in steady-state around normal operating point where small perturbations are applied to simulate the primary frequency response. Thus, only speed control and fuel-turbine dynamics will be considered. The generic low-order SFR model of a GPP is shown in Figure 2, where Δf, ΔP_m are the small change in frequency and active power, respectively. R_{GT}, T_g, T_{VP}, T_{FS} and T_{CD} are governor droop, governor servo time constant and time constants related to valve positioning, fuel dynamics and compressor discharge, respectively. Typical values of these constants are given in Table I.
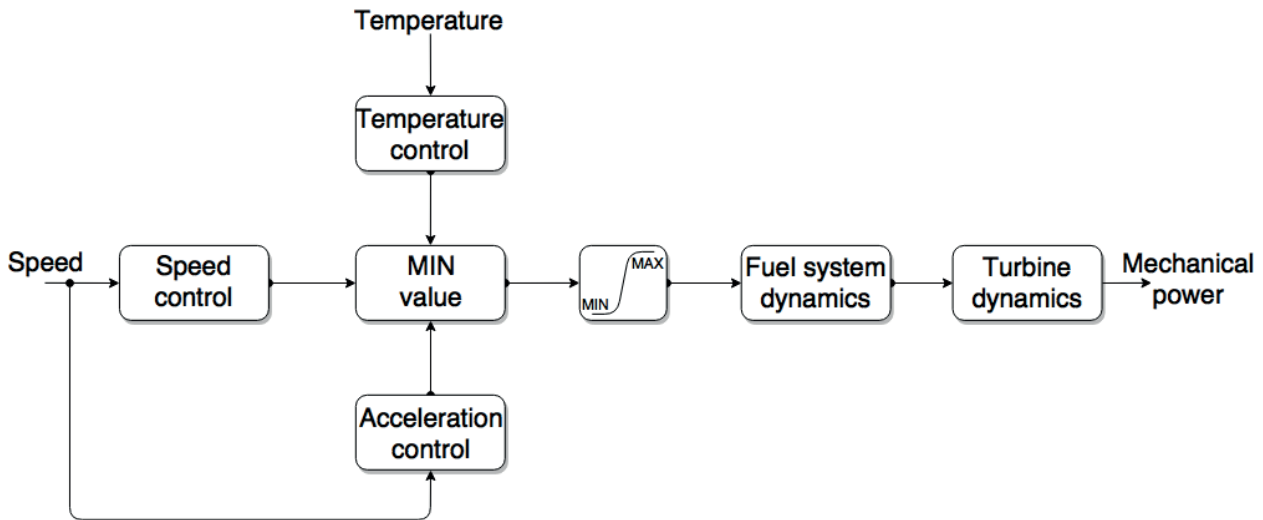
Figure 1. General gas turbine model for power system stability studies
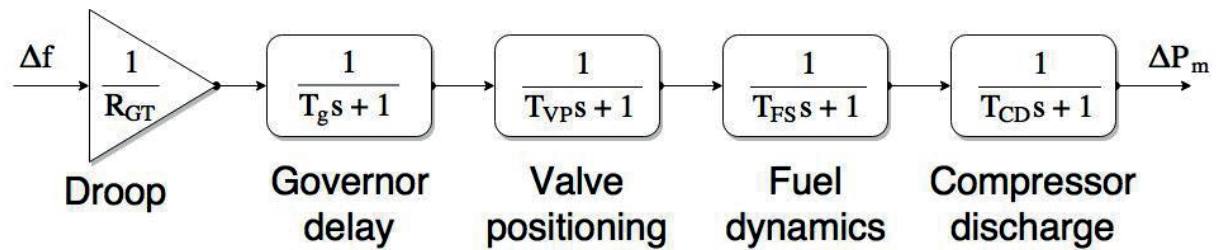
Figure 2. Gas power plant SFR model

Table I. Typical values of gas turbine parameters

According to:	R_{GT}	T_g [s]	T_{VP} [s]	T_{FS} [s]	T_{CD} [s]
Weimin *et al.* [10]	$3 - 6\%$	-	0,1	-	0,94
Zhang and So [12]	$2 - 10\%$	0,1	0,1	0,4	0,4

The difference in values can be explained by the fact that authors in [12] use standard IEEE governor models with typical recommended values, while authors in [10] used real gas turbine experimental data to identify the gas turbine parameters. A combined-cycle plant has been used in both [10] and [12].

3.   A GENERIC WIND TURBINE MODEL FOR SFR SIMULATIONS

Before the SFR model of a wind turbine is developed, it is necessary to classify different types of wind turbines since they have different characteristics and dynamic behavior which determine how those turbines are modelled. After the brief overview of wind turbine generator topologies, frequency support from wind turbines is briefly discussed. Finally, the general assumptions which the simplified modelling is based upon are laid down and the generic wind turbine SFR model is developed.

3.1. Overview of wind turbine generator topologies

Different wind turbine generator topologies are shown in Figure 3. The wind turbine itself doesn't differ between different topologies since horizontal axis wind turbines have the same blade design concept. The difference between wind turbine topologies comes from the generator-converter pair.
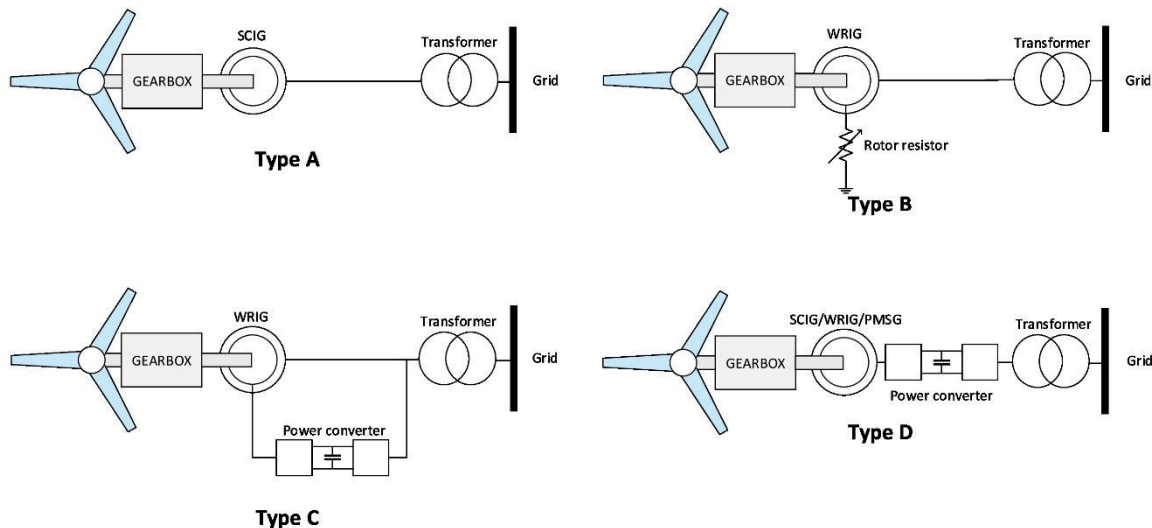
Figure 3. Wind turbine generator topologies

Type A is the fixed-speed wind turbine which utilizes a squirrel cage induction generator (SCIG). Rotor speed is quasi-fixed with the slip less than 1% and dictated by the grid frequency. Type A wind turbine is connected to the grid only through a transformer. Type B is the variable-slip wind turbine. It utilizes a wound rotor induction generator (WRIG) with a variable rotor resistor to control the slip between 0–10% in super-synchronous mode. It is also connected to the grid through a transformer.

Variable-speed wind turbines (VSWTs) can be divided into Type C (partially decoupled using partially rated frequency converter) and Type D (fully decoupled using fully-rated frequency converter). Both are connected to the grid through a power converter interface. The former topology is called a doubly-fed induction generator (DFIG) which uses a (WRIG), while the latter is in literature sometimes called full-scale converter (FSC) wind turbine generator which can utilize SCIG or permanent magnet synchronous generator (PMSG) for geared solutions; or PMSG and wound rotor synchronous generator (WRSG) for direct-drive solutions.

3.2. Grid frequency support provision from wind turbines

In this paper, the emphasis of frequency support is on the time scales of inertial response and primary frequency response. Capability of a wind turbine to provide frequency support depends on its topology. Type A and Type B wind turbines have inherent inertial response since they are directly connected to the grid. A spinning reserve can be obtained by pitch angle control in Type A and by

pitch angle control or variable rotor resistance in Type B [13], however the operating speed range is very limited, and it is difficult to control the spinning reserve with the pitch control, while the frequent use of rotor resistance generates more heat which is wanted minimized. Type C and D wind turbines are significantly more controllable, and the spinning reserve is achieved easier due to the power electronic interface. On the other hand, this power electronic interface, decouples the mechanical behavior of the turbine and electrical behavior on the grid side, thus removing the inertial response. More on inertial response and primary frequency control from wind turbines can be found in [13],[14]. Wind turbines do not usually participate in inertial or primary frequency response of a power system, but as the share of wind power in power systems worldwide keeps growing, system operators are recognizing the need to include WPPs in ancillary services related to frequency support and some have already implemented various measures[5].

3.3. Developing the wind turbine SFR model

Although Type A and Type B wind turbines still exist in power systems today, they are probably at the end of their life span and are being pushed out by types C and D due to their superior aerodynamic efficiency and controllability [4]. Therefore, in this paper, the focus is on VSWTs and they are the ones which will be modelled in the rest of the paper. WECS is a complex electromechanical system and the order and the type of modelling depends on the type of intended simulations. For power system dynamics & stability simulations (more precisely, for studying power system frequency changes by low-order SFR models in this case), certain assumptions have to be made which will enable the simplification and the reduction of the model order. These assumptions are very well documented in [15]–[18]:

- Rotor is modelled as a lumped-mass because shaft dynamics are hardly reflected on the grid side;
- flux dynamics in the stator and rotor voltage equations are neglected which results in algebraic generator equations. Therefore, the generator is modelled as an electrical torque source. Fast action of power electronic converters means the new set-point is reached almost instantaneously.

3.3.1. Rotor model

Mechanical power developed at the turbine shaft is expressed as:

$$P_m = \frac{1}{2}\rho R^2 \pi v^3 C_p(\lambda, \beta) \tag{1}$$

where ρ is the air density, R is the rotor radius, v is the wind speed, C_p is the aerodynamic coefficient which is a function of the pitch angle β and the tip-speed ratio λ. The tip-speed ratio is defined as the ratio of the blade tip velocity and the wind velocity:

$$\lambda = \frac{\omega_t R}{v} \tag{2}$$

where ω_t is the angular velocity of the turbine. A generic numerical expression for C_p from [17] is used:

$$C_p(\lambda, \beta) = 0.73 \left(\frac{151}{\lambda - 0.02\beta} - \frac{0.453}{\beta^3 + 1} - 0.58\beta - 0.002\beta^{2.14} - 13.2 \right) e^{-\left(\frac{18.4}{\lambda - 0.02\beta} - \frac{0.0552}{\beta^3 + 1} \right)}. \tag{3}$$

The $C_p - \lambda$ curves are shown in Figure 4 with pitch angle β in degrees as a parameter. It can be seen that for every pitch angle there exists an optimal tip-speed ratio for which the aerodynamic efficiency is maximized. This also holds true for every wind speed. Therefore, the generator speed is controlled in a way that will maximize the tip-speed ratio for a given wind speed. This is called maximum-power-point-tracking (MPPT).
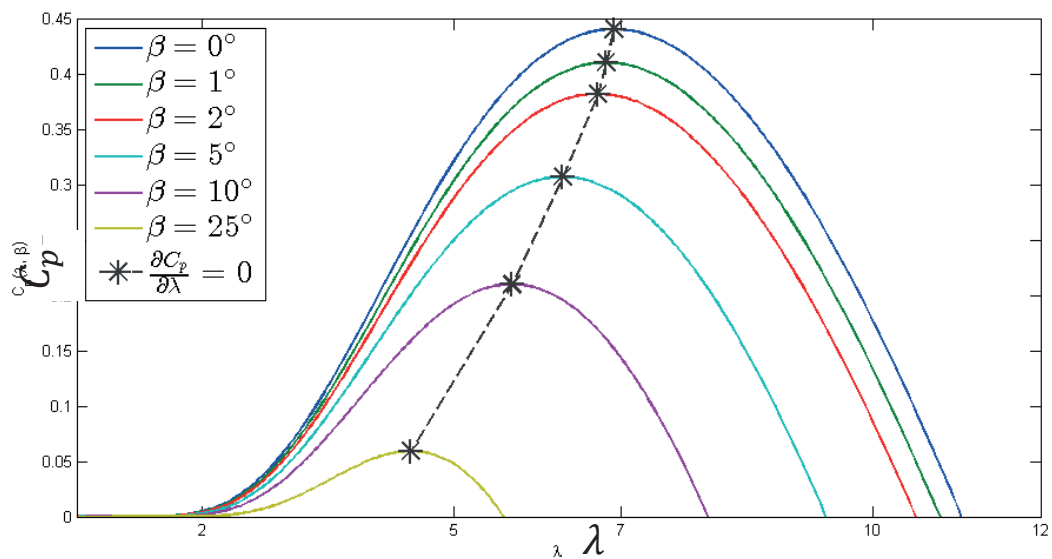
Figure 4. Graphical representation of $C_p - \lambda$ curves for β as a parameter [4]

In this paper, the achieved deloading has been achieved solely by pitch angle control and the extra active power injection after a disturbance is achieved by pitching the blades which most closely resembles a tradition turbine governing. However, this is not the most accurate approach nor the only approach: the wind turbine is controlled differently depending on the wind conditions [19], and the pitch angle controller is usually active only during high wind speeds. Moreover, a spinning reserve can be achieved by generator speed control during lower wind speeds. Nevertheless, to avoid taking into account different control modes, the pitch angle control has been chosen as a mechanism for primary frequency response of a wind turbine ignoring the actual wind conditions.

Generator power—rotor speed curve is described in [19] in more detail. Succinctly, it represents the control action by which the wind turbine generator speed and output power is controlled. The control action (e.g. minimum and maximum speed control, MPPT, power control) depends on the current wind conditions. However, in this paper, only MPPT mode is considered. Here, the generator power is proportional to the cube of generator speed

$$P_e = k_g \omega_g^3 - K_e \delta f \tag{4}$$

where k_g is the generator power—speed curve coefficient and ω_g is the generator mechanical (high-speed shaft) speed. The value of coefficient k_g depends on the turbine parameters, but also on the base values for which the equations are normalized in p.u. values. This MPPT curve is shown in Figure 5 for different wind speeds. This generator power reference is offset when a frequency disturbance δf occurs, with K_e being the gain of the proportional controller.
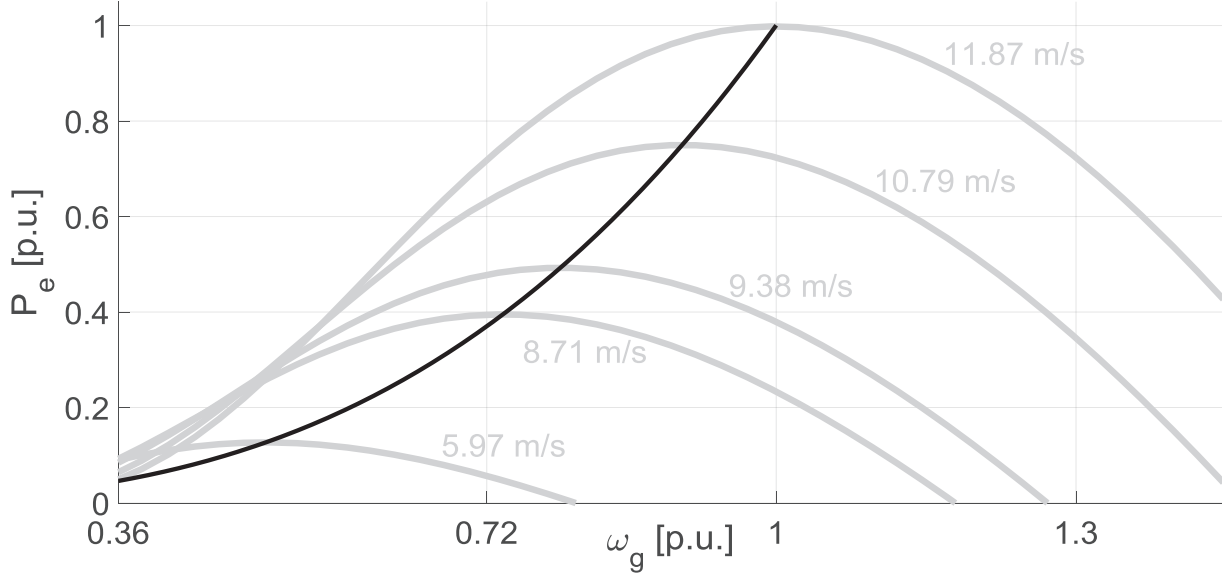
Figure 5. MPPT curve

Pitch angle is usually only active during high wind speeds to limit the aerodynamic torque exerted on the turbine, but here it will also be used to reserve a certain power margin and to control the pitch angle during a frequency disturbance. P controller is used instead of a PI controller to further simplify the model [17] and the pitch control servomechanism is modeled as a first-order lag as described by (5).

$$T_s \frac{d\beta}{dt} = -\beta + K_m \delta f \tag{5}$$

T_s is the servo time constant and the other half of frequency control is completed by the $K_m \delta f$ member, where K_m is the gain of the proportional controller. K_e and K_m can be considered analogous to the droop gain of conventional turbine systems, but here the former changes the generator setpoint, while the latter changes the mechanical power by controlling the aerodynamic torque.

The motion equation completes the wind turbine model:

$$2H_{WT} \frac{d\omega_g}{dt} = \frac{P_m - P_e}{\omega_g} \tag{6}$$

Rotor acts as a buffer and the high-frequency components of the wind speed signal is evened out over the rotor surface [18]:

$$T_W \frac{dv}{dt} = -v + u \tag{7}$$

where u is the raw wind speed signal, and low-pass filter time constant T_W is set to 4 seconds [18].

Equations (1), (4), (5), (6) and (7) represent the simplified mathematical model of the turbine. The aforementioned expressions are linearized around initial operating point to obtain the SFR model of a wind turbine. The state-space model is described by (8), (9), while the complete derivation can be found in [4]. Numerical values of coefficients $a_{1,1}$–$a_{1,3}$ and c_1–c_3 are given in the Table III in the Appendix.

$$
\begin{pmatrix} \Delta \dot{\omega}_t \\ \Delta \dot{\beta} \\ \Delta \dot{v} \end{pmatrix} = \mathbf{A} \begin{pmatrix} \Delta \omega_t \\ \Delta \beta \\ \Delta v \end{pmatrix} + \mathbf{B} \begin{pmatrix} \Delta f \\ \Delta u \end{pmatrix}
$$

$$
\Delta P_m = \mathbf{C} \begin{pmatrix} \Delta \omega_t \\ \Delta \beta \\ \Delta v \end{pmatrix} + \mathbf{D} \begin{pmatrix} \Delta f \\ \Delta u \end{pmatrix}
$$

(8)

$$
\mathbf{A} = \begin{pmatrix} \dfrac{a_{1,1}}{2H_{WT}} & \dfrac{a_{1,2}}{2H_{WT}} & \dfrac{a_{1,3}}{2H_{WT}} \\ 0 & -\dfrac{1}{T_s} & 0 \\ 0 & 0 & -\dfrac{1}{T_W} \end{pmatrix} \qquad \mathbf{B} = \begin{pmatrix} \dfrac{K_e}{2H_{WT}} & 0 \\ \dfrac{K_m}{T_s} & 0 \\ 0 & \dfrac{1}{T_W} \end{pmatrix}
$$

(9)

$$
\mathbf{C} = \begin{pmatrix} c_1 & c_2 & c_3 \end{pmatrix} \qquad\qquad \mathbf{D} = \begin{pmatrix} 0 & 0 \end{pmatrix}
$$

From (8), (9) the transfer function that represents the generic low-order SFR model of a VSWT is derived:

$$
\mathbf{G}(s) = \begin{pmatrix} K_m \dfrac{(2K_m(c_2 a_{11} - a_{12} c_1) - K_e c_1) - s(2K_m c_2 H_{WT} + K_e c_1 T_s)}{2(sT_s + 1)(a_{11} - sH_{WT})} \\ \dfrac{1}{sT_w + 1} \dfrac{c_3 a_{11} - a_{13} c_1 - c_3 H_{WT} s}{a_{11} - sH_{WT}} \end{pmatrix}
$$

(10)

4. EXPANDED SFR MODEL OF A POWER SYSTEM

The final goal of [4] was to expand the existing SFR model of a power system which includes a steam turbine [20] and a hydro turbine [9] so that it includes the gas turbine and a wind turbine as well. This model developed in MATLAB/Simulink environment is shown in Figure 6, and it also includes the dynamic demand response (DR) model [21] and the UFLS scheme. The used steam and hydro turbine models, as well as the UFLS model and DR model are shown in the Appendix.
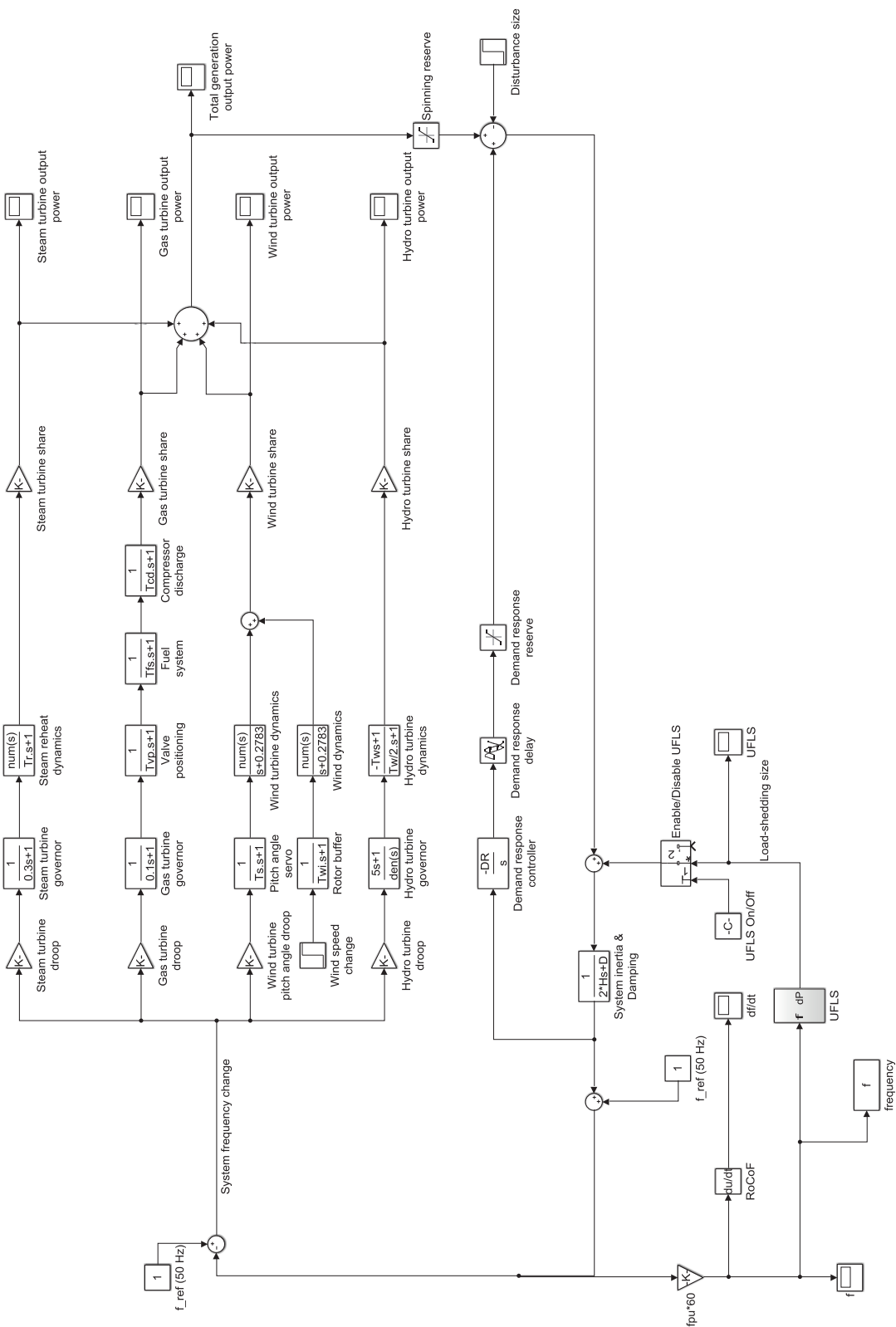
Figure 6. Expanded SFR model of a power system

4.1. Graphical user interface of the model

Graphical user interface has also been created in MATLAB GUIDE environment (Figure 7). It enables the user to easily change different parameters and run an arbitrary number of simulations while the results figures (system frequency and power output of power plants) are generated automatically (Figure 8).
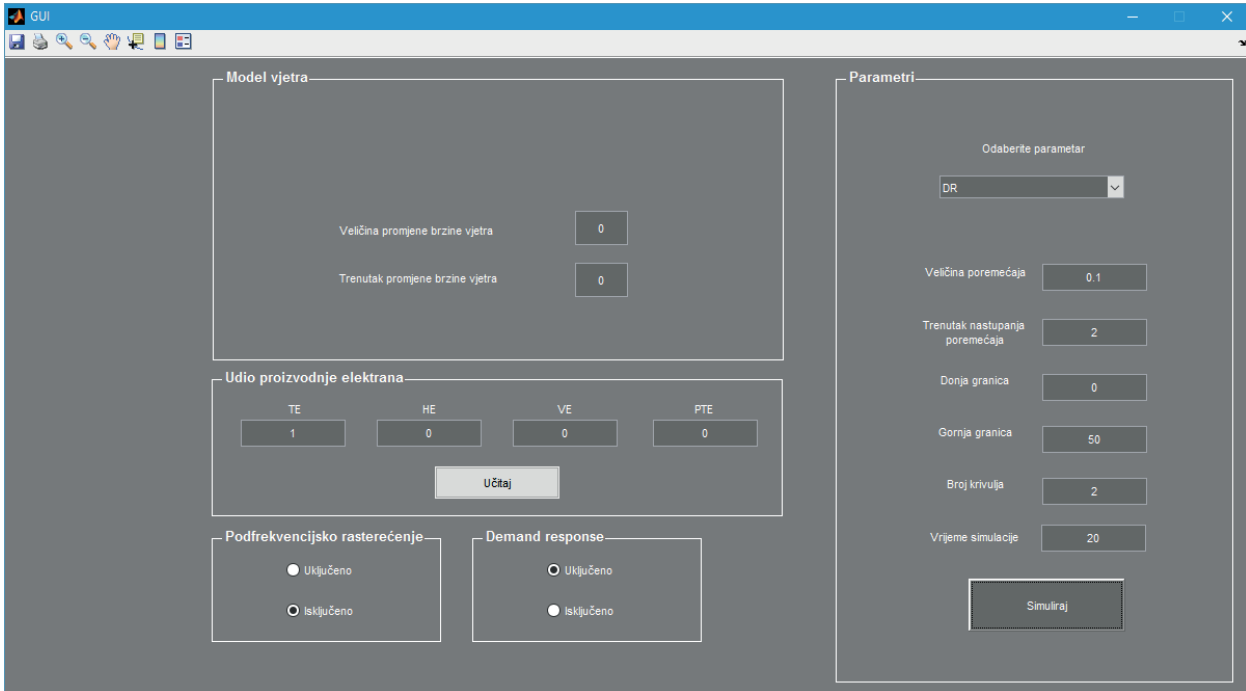
Figure 7. Screenshot of a graphical user interface of the developed model
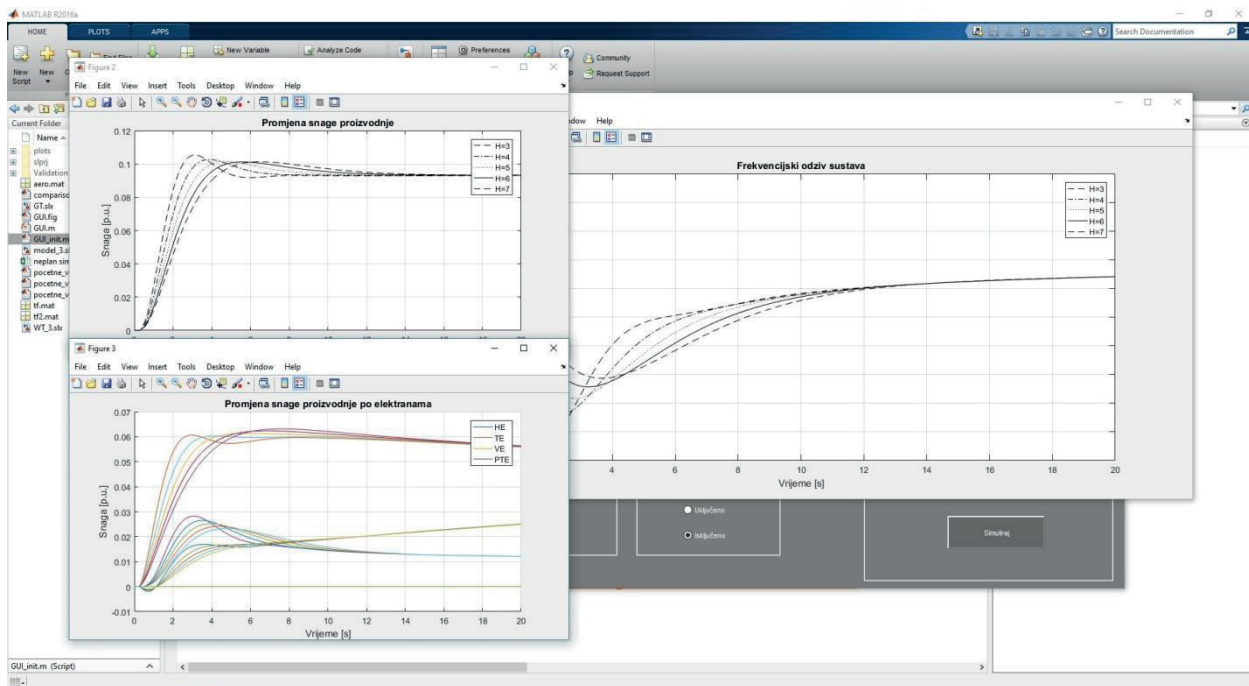
Figure 8. Screenshot of automatically generated figures

4.2. Simulation examples

Now, the presented SFR model can be used to study power system frequency dynamics for different operational scenarios (e.g. different generation mix, increase of wind power penetration, inertia reduction, etc.) and how different parameters influence the frequency dynamics (e.g. turbine droop, turbine time constants, etc.). Default simulation parameters are shown in Table II; if some parameter is changed during the simulations, the rest are held constant according to Table II.

Table II. Default simulation parameters

Steam turbine				Hydro turbine					Gas turbine				
R	T_2[s]	F_H	T_R[s]	R	T_W[s]	T_2[s]	T_3[s]	T_4[s]	R	T_g[s]	T_{VP}[s]	T_{FS}[s]	T_{CD}[s]
0.05	0.3	0.3	8	0.04	1	0.5	5	50	0.06	0.1	0.1	0.4	0.4
System			Demand response					Wind turbine					
H [s]	D	ΔP_D [p.u.]		K_{DR}			T_d [s]		H_{WT} [s]	K_m		K_e	T_s [s]
4	1	0.05		10			0.2		3	20		20	0.25

4.2.1. Impact of wind power share in the generation mix on the frequency response

Starting with a system with 50% hydro power and 50% thermal power (similar to the Croatian power system), the share of wind power capacity is increased in the increments of 5% (this is offset by the reduction of steam units), but the wind power plants do not have any frequency support capabilities. A load disturbance $\Delta P_D = 0.05$ p.u. is applied. From Figure 9, it can be seen that the increase of the wind power in the system worsens the frequency response of the system: nadir and steady-state error are larger.
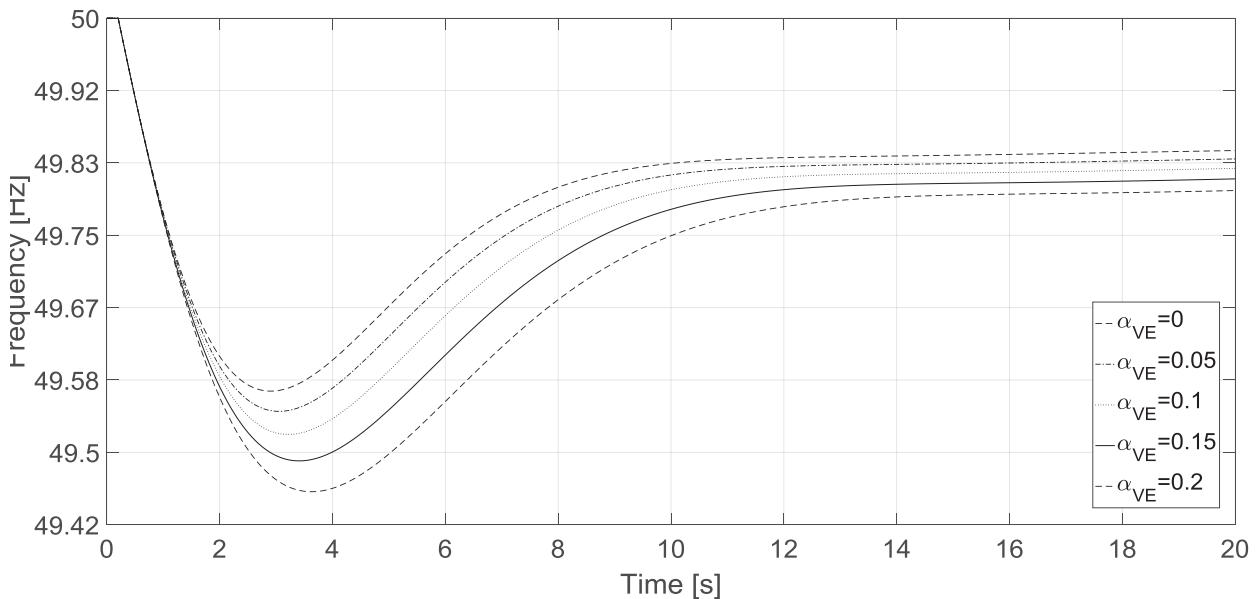
Figure 9. Frequency response of a system for different wind power penetration

4.2.2. Impact of participation of WPPs in primary frequency response

For a system with 40% thermal power, 40% hydro power and 20% wind power, the frequency response is studies for when there is no active power contribution from WPPs and for when the WPPs are deloaded 10% and they can inject extra active power after a disturbance. Results are shown in Figure 10. It can be seen that participation of WPPs in primary frequency response can significantly improve the system frequency response because the power set-point of a VSWT can be changed almost instantaneously. This is an illustrative example and the real contribution depends on WPP frequency controller gains as well as the instantaneous capability of WPPs to provide reserve power which depends on the wind conditions:

- if the wind speeds are too low they will not participate in frequency control;
- if the wind speeds are too high they will shut down to protect the turbine;
- the actual amount of power reserve may be lower since the 10% is quite high and a lot of wind energy is wasted in this case.
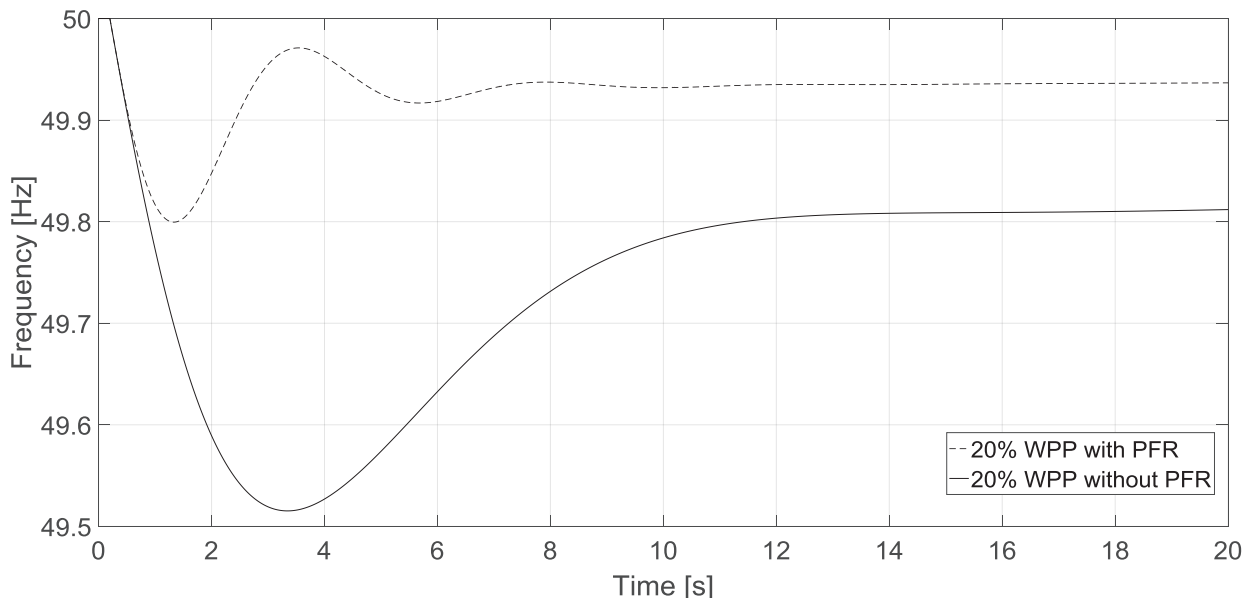
Figure 10. Impact of primary frequency response (PFR) from WPPs on system frequency

4.2.3. Impact of gas turbine share in the generation mix on the frequency response

Starting with a system with 50% hydro power and 50% thermal power, the share of gas power plants is increased in the increments of 5% (this is offset by the reduction of hydro units). From Figure 9, it can be seen that the increase of the gas turbines in the system reduces the frequency nadir since the gas turbines have a much faster response than hydro turbines, but also, hydro turbines are non-minimal phase shift systems due to the water inertia and the output power is reduced immediately after a disturbance which contributes to worse frequency response—gas turbines do not possess that characteristic.
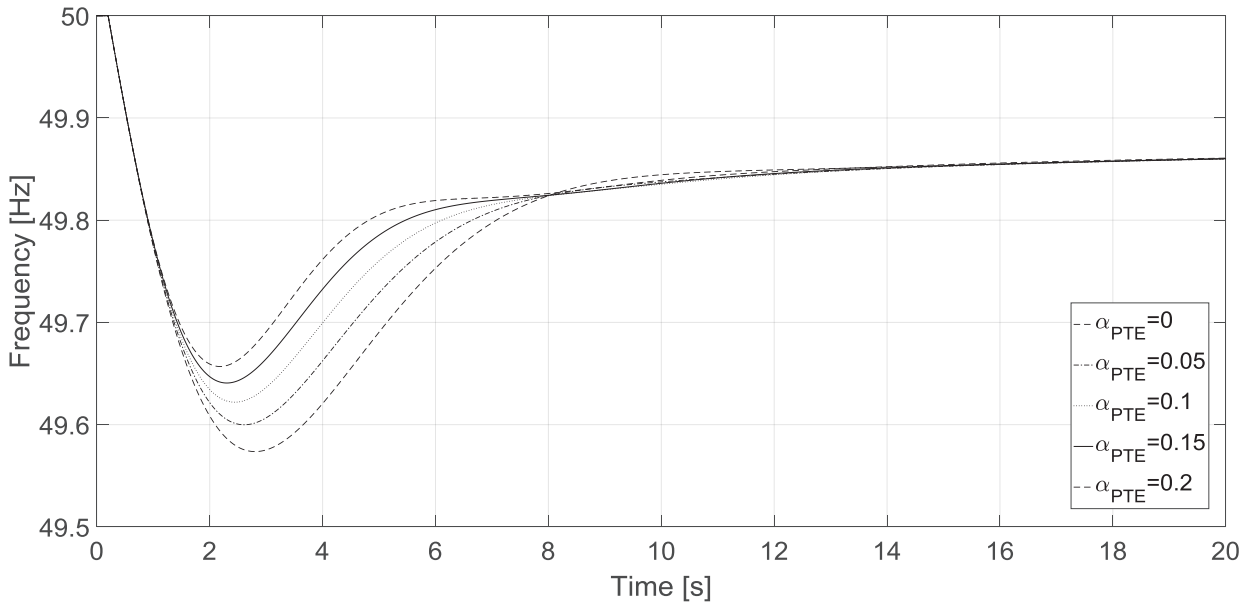
Figure 11. Impact of gas turbine share on frequency response

4.2.4. Impact of dynamic demand response on frequency response

Introduction of a dynamic demand response can improve frequency nadir and the steady-state error of frequency as seen in Figure 12. After a disturbance, smart, responsive loads lower their power consumption which can help in maintaining system stability. Some examples of these kinds of loads are electric water heaters or HVAC systems [21].
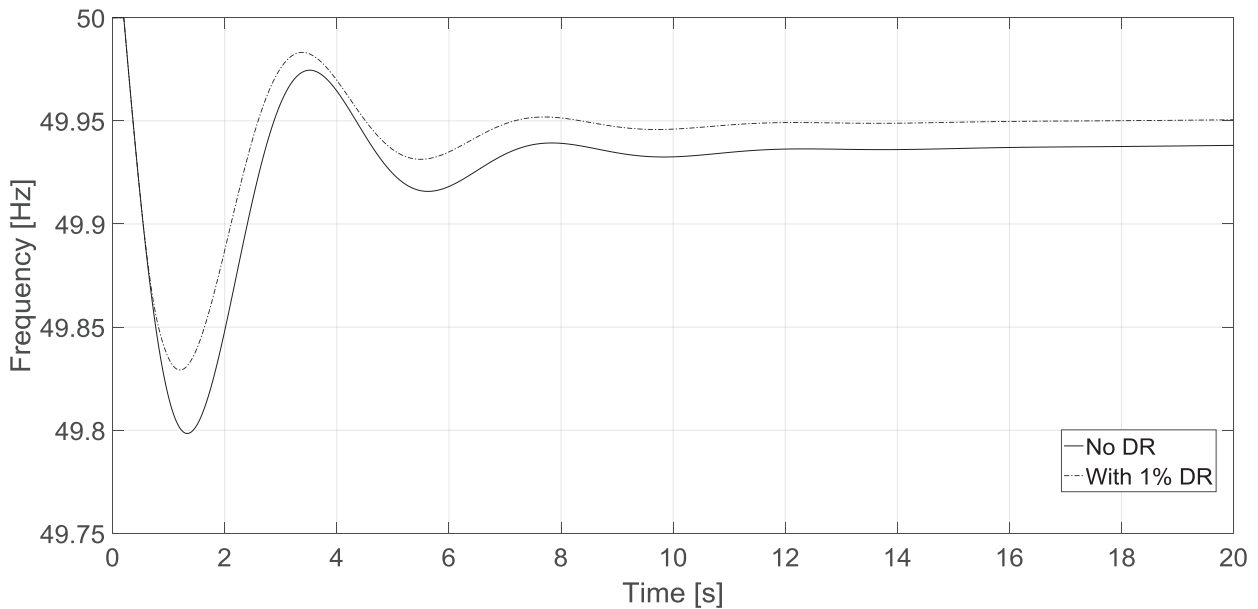
Figure 12. Impact of dynamic demand response on system frequency

5. CONCLUSION

This paper summarizes the main results of [4]. With the development of new energy technologies and smart grid technologies, power systems throughout the world are changing. Since not many power systems consist only of thermal or hydro units, the goal was to expand existing SFR model of a steam-hydro system to now include the gas turbines and wind turbines because their share is not anymore insignificant. Moreover, as smart, responsive loads also show great promise for balancing services, a dynamic model of a demand response has also been incorporated. Since modern wind turbines are converter-connected to the grid they are insensitive to changes in grid frequency. Therefore, a simplified model of a wind turbine which utilizes pitch angle control and generator-converter control to obtain an active power reserve which is injected to the grid upon an active power disturbance in the system by supplementary Δf control which is analogous to the turbine governor response for primary frequency control. The expanded SFR model now contains the 4 most common types of turbines (steam, hydro, gas and wind), dynamic demand response and an UFLS scheme to simulate load shedding. The SFR models are easy to implement and can be used to qualitatively study power system frequency changes without the need to model detailed grids in power system simulation software which requires knowledge of a lot of parameters. A graphical user interface has been created to quickly change simulation parameters, run numerous simulations and generate graphical results.

6. REFERENCES

[1]   International Renewable Energy Agency. "Renewable energy capacity statistics 2017", 2017. http://www.irena.org, accessed 12 November 2017.

[2]   U.S. Energy Information Administration. "International Energy Outlook 2017", 2017. https://www.eia.gov/outlooks/ieo/, accessed 3 January 2018.

[3]   J. G. Slootweg, S. W. H. de Haan, H. Polinder, and W. L. Kling, "General model for representing variable speed wind turbines in power system dynamics simulations," IEEE Trans. Power Syst., vol. 18, no. 1, pp. 144–151, 2003.

[4]   M. Krpan, "The mathematical and simulation model of a wind power plant and a gas power plant", master thesis, University of Zagreb Faculty of Electrical Engineering and Computing, September 2016.

[5]   M. Krpan and I. Kuzle, "Inertial and primary frequency response model of variable-speed wind turbines," *Publ. J. Eng.*, 2017.

[6]   M. Krpan and I. Kuzle, "Linearized model of variable speed wind turbines for studying power system frequency changes," in *17th IEEE International Conference on Smart Technologies, EUROCON 2017 - Conference Proceedings*, 2017.

[7]   Z. Wu *et al.*, "State-of-the-art review on frequency response of wind power plants in power systems," *J. Mod. Power Syst. Clean Energy*, Sep. 2017.

[8] P. M. Anderson and M. Mirheydar, "A low-order system frequency response model," *IEEE Trans. Power Syst.*, vol. 5, no. 3, pp. 720–729, 1990.

[9] I. Kuzle, T. Tomisa, and S. Tesnjak, "A mathematical model for studying power system frequency changes," *IEEE AFRICON Conf.*, vol. 2, Gaborone, Botswana, pp. 761–764, 2004.

[10] K. Weimin, X. Junrong, G. Lian, and D. Yiping, "Study on the mathematical model and primary frequency regulation characteristics of combined cycle plants," *2011 Second Int. Conf. Mech. Autom. Control Eng.*, pp. 2632–2635, 2011.

[11] P. Centeno, I. Egido, and C. Domingo, "Review of gas turbine models for power system stability studies," *9th Spanish Port. Congr. Electr. Eng.*, pp. 1–6, 2005.

[12] Q. Zhang and P. L. So, "Dynamic modelling of a combined cycle plant for power system stability studies," *Power Eng. Soc. Winter Meet. 2000. IEEE*, vol. 2, no. c, pp. 1538–1543 vol.2, 2000.

[13] E. Muljadi, M. Singh, and V. Gevorgian, "Fixed-speed and variable-slip wind turbines providing spinning reserves to the grid," *IEEE Power Energy Soc. Gen. Meet.*, no. November 2012, 2013.

[14] E. Muljadi, V. Gevorgian, and M. Singh, "Understanding Inertial and Frequency Response of Wind Power Plants," *2012 IEEE Power Electron. Mach. Wind Appl.*, no. July, pp. 1–8, 2012.

[15] J. G. Slootweg, H. Polinder, and W. L. Kling, "Dynamic modelling of a wind turbine with doubly fed induction generator," *2001 Power Eng. Soc. Summer Meet. Conf. Proc. (Cat. No.01CH37262)*, vol. 1, pp. 644–649 vol.1, 2001.

[16] J. G. Slootweg, H. Polinder, and W. L. Kling, "Dynamic modeling of a wind turbine with direct drive synchronous generator and back to back voltage source converter," *Conf. Eur. Wind Energy Conf. Copenhagen*, July, 2001.

[17] J. G. Slootweg, S. W. H. de Haan, H. Polinder, and W. L. Kling, "General model for representing variable speed wind turbines in power system dynamics simulations," *IEEE Trans. Power Syst.*, vol. 18, no. 1, pp. 144–151, 2003.

[18] J. G. Slootweg, H. Polinder, and W. L. Kling, "Representing Wind Turbine Electrical Generating Systems in Fundamental Frequency Simulations," *IEEE Trans. Energy Convers.*, vol. 18, no. 4, pp. 516–524, 2003.

[19] G. Abad, J. Lopez, M. A. Rodriguez, L. Marroyo, and G. Iwanski, *Doubly fed induction machine: modeling and control for wind energy generation*, 1st ed. John Wiley & Sons, 2011.

[20] M. Lukic, I. Kuzle and S. Tesnjak, "An Adaptive Approach to setting Underfrequency Load Shedding Relays for an Isolated Power System with Private Generation," IEEE MELECON '98, Tel-Aviv, Israel, pp. 1122–1125, 1998.

[21] S. A. Pourmousavi and M. H. Nehrir, "Introducing dynamic demand response in the LFC model," *IEEE Trans. Power Syst.*, vol. 29, no. 4, pp. 1562–1572, 2014.

7. APPENDIX

7.1. Numerical values of linearized wind turbine model

Linearization of the presented wind turbine model includes some parameters that depend on the initial condition around which the model is linearized. Due to the high complexity (nonlinearity) of the mathematical expressions, only numerical values are given. These parameters are shown in Table III. The definition of these parameters is given in [4] and are not repeated here, but they originate during the Taylor's series expansion neglecting higher order terms during the linearization process.

Table III. Numerical values of the SFR wind turbine model parameters [4]

v [p.u.]	$a_{1,1}$	$a_{1,2}$	$a_{1,3}$	c_1	c_2	c_3
0.9	-1.1273	-0.0100	1.0547	-0.7233	-0.0200	2.1093
0.95	-1.2550	-0.0118	1.1751	-0.8064	-0.0236	2.3502
1.00	-1.3913	-0.0138	1.3021	-0.8931	-0.0275	2.6041
1.05	-1.5346	-0.0159	1.4355	-0.9843	-0.0318	2.8710
1.1	-1.6832	-0.0183	1.5755	-1.0809	-0.0366	3.1510

7.2. Steam reheat turbine model, hydro turbine model, dynamic demand response model and UFLS scheme model.
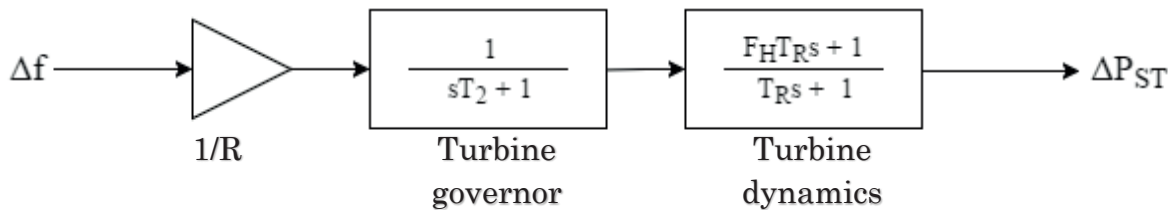
Figure 13. SFR model of a steam reheat turbine
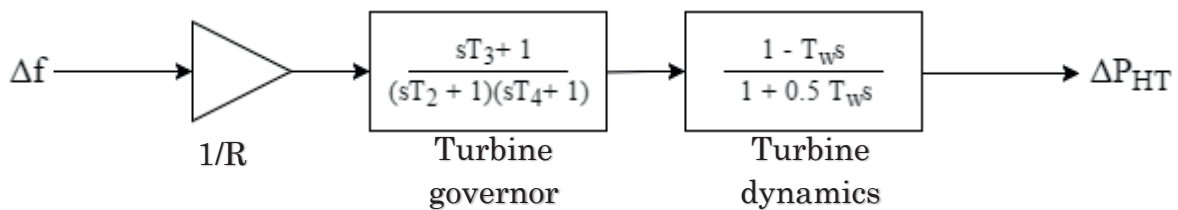
Figure 14. SFR model of a hydro turbine

Table IV. Typical values of turbine parameters [4]

Steam	R	T_2 [s]	F_H	T_R [s]	
	$2\% - 7\%$	$0.2 - 0.3$	0.3	$4 - 11$	
Hydro	R	T_2 [s]	T_3 [s]	T_4 [s]	T_w [s]
	$2\% - 4\%$	0.5	5	50	$0.5 - 5$
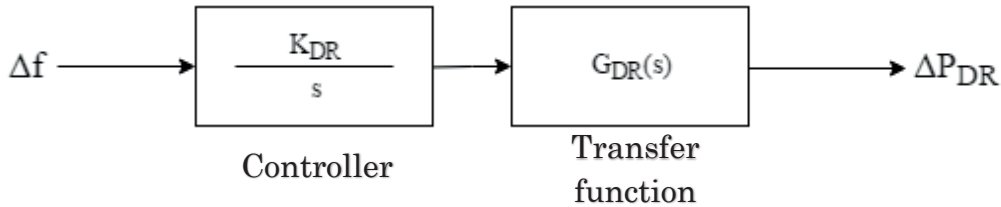
Figure 15. Dynamic demand response model of a hydro turbine

$G_{DR}(s)$ represents an 2nd order approximation of the transport delay e^{-sT_d} [21]:

$$G_{DR}(s) = \frac{\dfrac{3360}{T_d^3}s^2 - \dfrac{15120}{T_d^4}s + \dfrac{30240}{T_d^5}}{\dfrac{3360}{T_d^3}s^2 + \dfrac{15120}{T_d^4}s + \dfrac{30240}{T_d^5}} \tag{11}$$

where $T_d \leq 0.5$ s and K_{DR} is arbitrary.
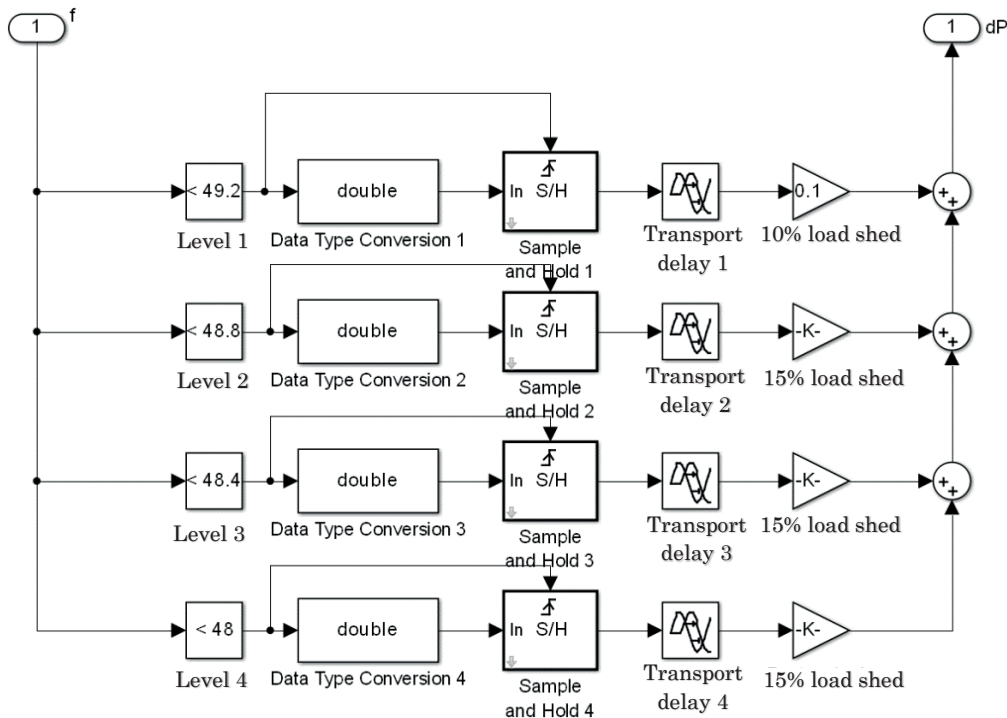
Figure 16. UFLS model in Simulink

UFLS transport delay is set to 400 ms which simulates circuit breaker action and under/frequency relays are set according to the Croatian grid code.